01.1

Impedance of a thin-film lithium-ion battery Si@O@Al—LiPON—$LiCoO_2$ at temperatures from -20°C to $+50^\circ$C

© A.S. Rudy, S.V. Kurbatov, A.A. Mironrenko, V.V. Naumov, Yu.S. Egorova

Demidov State University, Yaroslavl, Russia
E-mail: rudy@uniyar.ac.ru

Received November 16, 2022
Revised January 17, 2023
Accepted January 19, 2023

The results on measuring the impedance of a solid-state thin-film lithium-ion battery of the Si@O@Al−LiPON−$LiCoO_2$ electrochemical system in the temperature range from -20°C to $+50^\circ$C are presented. A structural model is proposed and the parameters of its elements, providing the best fit for the experimental Nyquist diagrams, are calculated. It is shown that the main contribution to the internal resistance is made by the LiPON-LiCoO2 interface. Based on the temperature dependence of the LiPON solid electrolyte conductivity the activation energy of lithium is determined, which is in good agreement with the literature data.

Keywords: Nanocomposite, lithium-ion battery, impedance spectroscopy, structural model, ionic conductivity.

DOI: 10.21883/TPL.2023.04.55869.19431

Solid-state thin-film lithium-ion batteries (SSTFLIBs) for portable and wearable electronics have become widespread in recent years. Their miniaturization was made possible by the use of thin-film technology and a solid electrolyte (lithium phosphorus oxynitride, LiPON). Unfortunately, the discharge capacity of SSTFLIBs is lower than the one typical of a battery with a liquid electrolyte, and their operating temperature range is narrower. The root cause of these restrictions has become evident as early as 2000, when Bates et al. found that the internal resistance of Li—LiPON—$LiCoO_2$ SSTFLIBs is produced primarily by the interfaces between functional layers [1]. This research paved the way for a series of studies focused on reducing the internal resistance of SSTFLIBs. The development of their structural models became an integral part of such studies. Batteries with negative electrodes made from lithium and graphite and a lithium cobaltite positive electrode were examined most often. Batteries with silicon electrodes remained almost uninvestigated, since the stability of crystalline silicon is low. The Si@O@Al—LiPON—$LiCoO_2$ electrochemical system, where the negative electrode is made of a high-capacity nanocomposite material (Si@O@Al), is of the utmost interest in this context. In the present study, we report the results of analysis and interpretation of impedance spectra of Si@O@Al—LiPON—$LiCoO_2$ SSTFLIBs.

Test SSTFLIB samples were produced by magnetron sputtering using an SCR 561 Tetra setup (Alcatel, France). The batteries had a multilayer structure: Si@O@Al ($0.3\,\mu$m)—LiPON ($1\,\mu$m)—$LiCoO_2$ ($1\,\mu$m)—Ti($10\,\mu$m), where Ti is the bottom layer. Their impedance was measured at temperatures ranging from -20 to $+50^\circ$C with a single-channel Elins P-40X potentiostat using the two-electrode setup. The voltage relative to a normally open circuit was 0 mV, the oscillation amplitude was 5 mV, and the frequency varied from 500 kHz to 50 mHz. Impedance measurements were carried out for batteries in discharged and charged states. Following a charge–discharge cycle, the sample was held at a certain temperature for 30 min, and its impedance was measured after that. The results of impedance spectroscopy were presented in the form of Nyquist diagrams.

Nyquist diagrams for each SSTFLIB state in the indicated temperature range take the form of a set of curves that are similar in shape. Only the resistance range changes with increasing temperature: Re(Z) varies from 21 000 Ω at -20°C to 140 Ω at $+50^\circ$C, while Im(Z) varies from 2000 Ω at -20°C to 70 Ω at $+50^\circ$C. Impedance spectra do not differ in any significant way from the spectra presented in [2–5]. The structural model shown in Fig. 1 was used to simulate impedance spectra. This model features a sequence of active resistances R and constant-phase elements (CPEs) connected in parallel. Solid electrolyte LiPON is presented in Fig. 1 in the form of a constant-phase element, which is a rather formal approximation. As was demonstrated in [6], it may be substituted by an equivalent circuit with ideal structural elements only. In the present study, CPEs are used just for convenience of comparison with the results reported elsewhere.

Element R_{NE} in Fig. 1 serves to model the drift charge transport in the Si@O@Al negative electrode, and $\mathrm{CPE_{NE}}$ reproduces its diffusion-capacitive conductivity. Likewise, R_{Elt} is the active resistance of an electrolyte and CPE_{Elt} is its diffusion-capacitive conductivity; R_{PE} is the active resistance of $LiCoO_2$ and $\mathrm{CPE_{PE}}$ is the diffusion-capacitive conductivity of $LiCoO_2$; $R_{Elt-Eld}$ models the drift charge transport through the LiPON—$LiCoO_2$ interface, and $\mathrm{CPE}_{Elt-Eld}$ models the diffusion-capacitive conductivity of the interface. The capacitive component of conductivity of the interface is produced by the dense part of the

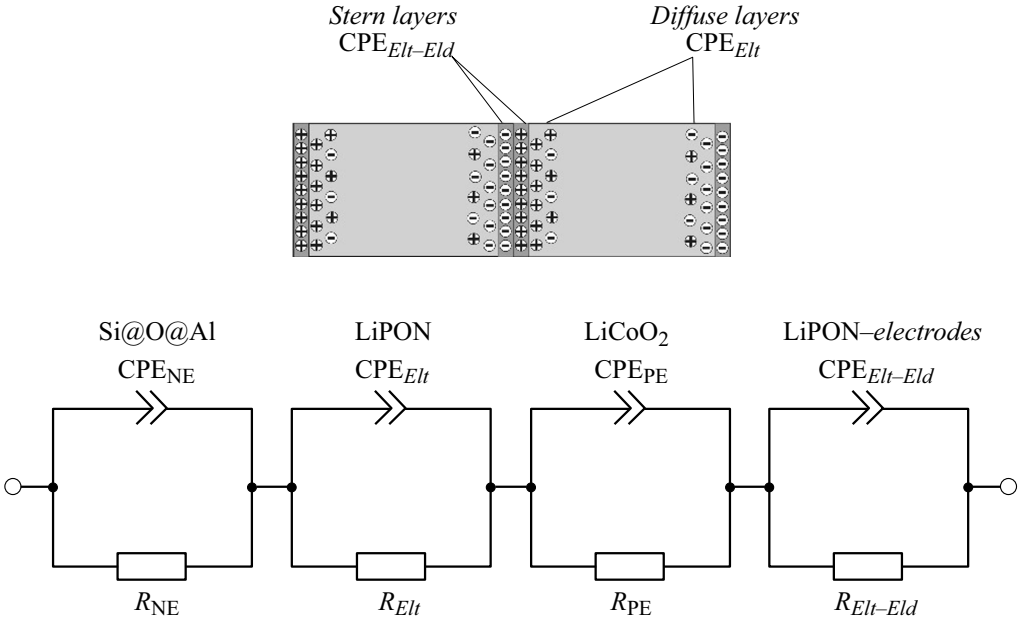

Figure 1. Structural model and equivalent circuit of the SSTFLIB. The following indices are used to denote structural elements: NE — negative electrode, Elt — electrolyte, PE — positive electrode, and $Elt-Eld$ — electrolyte−electrode interface.

electrical double layer (EDL, or Stern layer; see Fig. 1). The diffuse EDL part in the structural model represents the capacitive bulk component.

Similar circuits were used to simulate the impedance of an SSTFLIB of the Li—LiPON—$LiCoO_2$ electrochemical system [2–5] and lithium cobaltite [7]. However, they differ in certain respects. Specifically, a structural element representing the LiPON—$LiCoO_2$ interface impedance was missing in [3]. At the same time, a Warburg element was introduced into the LiPON circuit, although a CPE present there should suffice on its own. The impedance of interfaces of a solid electrolyte and electrodes is taken into account in the structural model in [4]. Notably, the diffusion properties of an electrolyte are modeled by a separate Warburg element, which is connected in series with structural elements of all functional layers. A capacitor, which models the current in a battery at constant voltage, is introduced into the structural model to simulate the so-called electrochemical capacitance. This capacitance is neglected in the model in Fig. 1 due to the boundedness of the frequency range.

The real and imaginary parts of impedance of the structural model take the form

$$\mathrm{Re}(\hat{Z}) = \sum_{n=1}^{4} R_n \frac{R_n A_n \omega^{\alpha_n} \cos\left(\alpha_n \frac{\pi}{2}\right) + A_n^2}{R_n^2 \omega^{2\alpha_n} + 2R_n A_n \cos\left(\alpha_n \frac{\pi}{2}\right) \omega^{\alpha_n} + A_n^2}, \quad (1)$$

$$\mathrm{Im}(\hat{Z}) = -j \sum_{n=1}^{4} \frac{R_n^2 A_n \omega^{-\alpha_n} \sin\left(\alpha_n \frac{\pi}{2}\right)}{R_n^2 + 2R_n A_n \omega^{-\alpha_n} \cos\left(\alpha_n \frac{\pi}{2}\right) + A_n^2 \omega^{-2\alpha_n}}, \quad (2)$$

where n is the order number of an $R-$CPE loop in Fig. 1, ω is the cyclic frequency, α is the nonideality factor, and A is the CPE amplitude. Nyquist diagrams for the SSTFLIB impedance in charged and discharged states at a temperature of $+20^\circ$C are presented in Fig. 2 to illustrate the accuracy of approximation of experimental curves. The results of approximation with the proposed model (formulae (1), (2)) are shown in the same figure for comparison. The best fit between the approximating dependence and experimental data is achieved at parameter values that are listed in the table.

The values of fitting parameters provide data on changes in functional SSTFLIB layers induced by their lithiation or delithiation. Specifically, the active resistance of Si@O@Al is somewhat higher in its nonlithiated state, since lithiated Si@O@Al is an electron semiconductor. Its ionic conductivity is of a diffusion-capacitive nature, which is evidenced by a nonideality factor of 0.77−0.78. The reduction in lithium concentration in the process of delithiation results in a 3-fold enhancement of diffusion-capacitive resistance A_{NE}.

It was demonstrated in [8] that the resistance of lithium cobaltite $Li_{1-x}CoO_2$ depends strongly on lithium deficiency x. The conductivity increase was attributed in [9,10] to the formation of holes in the $3d$ band. The conductivity variation is the key criterion for matching the resistances of 670 and 1170 Ω (see the table) with lithium cobaltite. Notably, diffusion-capacitive conductivity $A_{PE} \sim 2 \cdot 10^4\ \Omega/\mathrm{s}^{\alpha_{PE}}$ of lithium cobaltite undergoes no substantial changes in the course of delithiation, although the nature of ionic conductivity changes: it is largely diffusion-type in $LiCoO_2$ ($\alpha_{PE} = 0.66$), but shifts to a predominantly capacitive type in $Li_{1-x}CoO_2$ ($\alpha_{PE} = 0.79$).

Resistance $R_{Elt-Eld}$, which assumes a value of $\sim 10^5\ \Omega$, is the $LiCoO_2-$LiPON interface resistance that is induced by two factors. The first of them is the formation of an

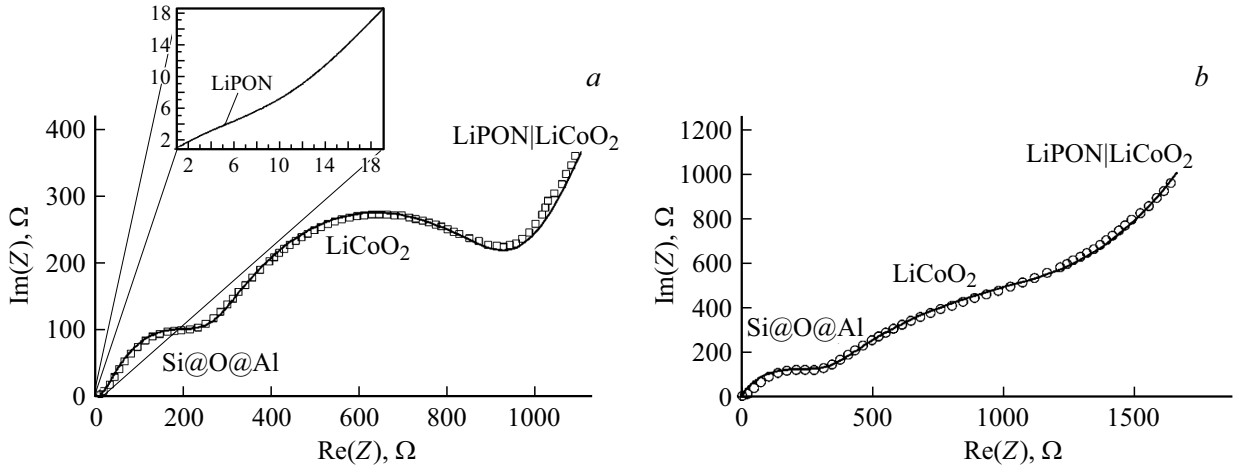

Figure 2. Results of fitting of the SSTFLIB impedance parameters. *a* — For a charged battery, *b* — for a discharged battery.

Parameters of approximating dependences (1) and (2) at +20°C

R_{Elt}, Ω	A_{Elt}, $\Omega/s^{1/2}$	α_{Elt}	R_{NE}, Ω	A_{NE}, $\Omega/s^{\alpha_{NE}}$	α_{NE}	R_{PE}, Ω	A_{PE}, $\Omega/s^{\alpha_{PE}}$	α_{PE}	$R_{Elt-Eld}$, Ω	$A_{Elt-Eld}$, $\Omega/s^{\alpha_{Elt-Eld}}$	$\alpha_{Elt-Eld}$
Charged battery											
15	$2.2 \cdot 10^4$	0.5	230	$2.2 \cdot 10^5$	0.77	670	$2 \cdot 10^4$	0.79	10^5	570	0.67
Discharged battery											
20	$2.2 \cdot 10^4$	0.5	270	$6.5 \cdot 10^5$	0.78	1170	$2.2 \cdot 10^4$	0.66	10^5	4500	0.77

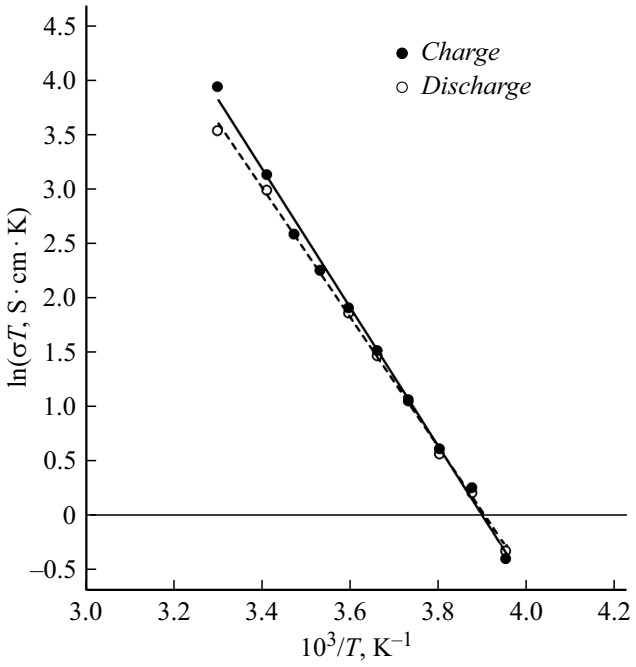

Figure 3. Experimental (points) and approximating (solid and dashed lines correspond to charge and discharge, respectively) dependences of conductivity of solid electrolyte LiPON.

extensive space charge region in the process of equalization of electrochemical potentials of the electrode and the electrolyte [11]. The second factor is the passivation layer that forms on contact of $LiCoO_2$ with atmosphere in the process of changing the mask. It is characteristic that the diffusion-capacitive resistance of the interface increases significantly (from 570 to 4500 $W/s^{\alpha_{Elt-Eld}}$) in the discharged state, while the conductivity becomes more capacitive in nature.

The results of fitting of SSTFLIB parameters provide an opportunity to determine temperature dependence $\sigma_{Elt}(T)$ of the electrolyte conductivity. Figure 3 presents experimental dependences $\ln(\sigma_{Elt}T) = f(1/T)$ and plots of the Arrhenius equation $\ln(\sigma_{Elt}T) = \ln\sigma_0 - E_a/k_BT$, where E_a is the activation energy of Li conductivity, k_B is the Boltzmann constant, T is absolute temperature, and σ_0 is a constant. The best fit between these dependences is obtained at $E_a = 0.55$ eV in the charged SSTFLIB state and at $E_a = 0.51$ eV in the discharged state. According to literature data, the activation energy of lithium conductivity in LiPON falls within the 0.40–0.57 eV range [5,12,13]. This agrees with the obtained results.

Thus, the proposed structural model provides an adequate description of impedance spectra of the SSTFLIB of the Si@O@Al–LiPON–$LiCoO_2$ electrochemical system within the entire temperature range of measurements and may be regarded as an equivalent circuit of this battery. The

model has an advantage in the structural similarity of models of individual SSTFLIB layers, which makes it possible to compare their parameters. The values of LiPON resistance and the corresponding activation energy of conductivity of lithium ions agree closely with literature data. The conductivity of nanocomposite Si@O@Al and $LiCoO_2$ corresponds to the results of measurements of test structures Ti—Si@O@Al—Ti and Ti—$LiCoO_2$—Ti. However, the values of $LiCoO_2$ resistivity deviate (depending on lithium deficiency) from those reported in [8]. The results of analysis of impedance spectra suggest that the internal SSTFLIB resistance is limited primarily by the LiPON—$LiCoO_2$ interlayer resistance. In order to reduce the internal SSTFLIB resistance, one should cut the contact of functional layers with atmosphere in the process of mask changing. The nature and structure of EDL in the LiPON—$LiCoO_2$ contact region also needs to be studied.

Funding

The study was supported financially by the Ministry of Science and Higher Education of the Russian Federation under state assignment No. 0856-2020-0006 for the Demidov Yaroslavl State University.

Conflict of interest

The authors declare that they have no conflict of interest.

References

[1] J.B. Bates, N.J. Dudney, B.J. Neudecker, F.X. Hart, H.P. Jun, S.A. Hackney, J. Electrochem. Soc., **147** (1), 59 (2000). DOI: 10.1149/1.1393157
[2] Y. Iriyama, T. Kako, C. Yada, T. Abe, Z. Ogumi, J. Power Sources, **146** (1-2), 745 (2005). DOI: 10.1016/j.jpowsour.2005.03.073
[3] Y. Iriyama, T. Kako, C. Yada, T. Abe, Z. Ogumi, Solid State Ionics, **176** (31-34), 2371 (2005). DOI: 10.1016/j.ssi.2005.02.025
[4] S.D. Fabre, D. Guy-Bouyssou, P. Bouillon, F. Le Cras, C. Delacourta, J. Electrochem. Soc., **159** (2), A104 (2012). DOI: 10.1149/2.041202jes
[5] S. Larfaillou, D. Guy-Bouyssou, F. Le Cras, S. Franger, ECS Trans., **61** (27), 165 (2014). DOI: 10.1149/06127.0165ecst
[6] A. Rudy, A. Mironenko, V. Naumov, A. Novozhilova, A. Skundin, I. Fedorov, Batteries, **7** (2), 21 (2021). DOI: 10.3390/batteries7020021
[7] D. Aurbach, M.D. Levi, E. Levi, H. Teller, B. Markovsky, G. Salitra, U. Heider, L. Heider, J. Electrochem. Soc., **145** (9), 3024 (1998). DOI: 10.1149/1.1838758
[8] D.G. Kellerman, V.R. Galakhov, A.S. Semenova, Ya.N. Blinovskov, O.N. Leonidova, Phys. Solid State, **48** (3), 548 (2006). https://journals.ioffe.ru/articles/viewPDF/3349 [D.G. Kellerman, V.R. Galakhov, A.S. Semenova, Ya.N. Blinovskov, O.N. Leonidova, Phys. Solid State, **48** (3), 548 (2006). DOI: 10.1134/S106378340603022X].
[9] E. Pichta, M. Solomon, S. Slane, M. Uchiyama, D. Chua, W.B. Ebner, H.W. Lin, J. Power Sources, **21** (1), 25 (1987). DOI: 10.1016/0378-7753(87)80074-5
[10] K. Wang, J. Wan, Y. Xiang, J. Zhu, Q. Leng, M. Wang, L. Xu, Y. Yang, J. Power Sources, **460**, 228062 (2020). DOI: 10.1016/j.jpowsour.2020.228062
[11] R. Hausbrand, *Surface science of intercalation materials and solid electrolytes*. Ser. SpringerBriefs in Physics (Springer, Cham, 2020). DOI: 10.1007/978-3-030-52826-3
[12] Y. Su, J. Falgenhauer, A. Polity, T. Leichtweiß, A. Kronenberger, J. Obel, S. Zhou, D. Schlettwein, J. Janek, B.K. Meyer, Solid State Ionics, **282**, 63 (2015). DOI: 10.1016/j.ssi.2015.09.022
[13] C.-L. Li, Z.-W. Fu, J. Electrochem. Soc., **154** (8), A784 (2007). DOI: 10.1149/1.2746550